Vol. 14 № 1 Trans. Nonferrous Met. Soc. China Feb. 2004

Article ID: 1003-6326(2004)01-0071-07

Coupled macro-micro modeling for prediction of grain structure of Al alloy①

XU Qing-yan(许庆彦), FENG Wei-ming(冯伟明), LIU Bai-cheng(柳百成)
(Department of Mechanical Engineering, Tsinghua University, Beijing 100084, China)

Abstract: A 3D stochastic modeling was presented to simulate the dendritic grains during solidification process of aluminum alloy. Shape functions were proposed in 2D and 3D to describe equiaxed dendritic shape. A growth model was presented to describe the growth of a nucleated grain and the capturing of the neighboring cells. On growing, each grain continues to capture the nearest neighboring cells to form the final grain shape. If a neighboring cell has been captured by other grains, the growth along this direction stops, which can reflect the grains impingement phenomenon occurring in solidification process. 2D and 3D calculations were performed to simulate the evolution of equiaxed dendritic grains. In order to verify the modeling results, step-shaped sample castings were cast in sand mold. The microstructure in various positions of the sample was observed. In addition the quantitative metallographic analysis also has been done to evaluate the grain size. Experimental and numerical results agree well.

Key words: Al alloy; stochastic modeling; microstructure simulation; equiaxed dendritic grain

CLC number: TG 21 **Document code:** A

1 INTRODUCTION

The grain structure has a direct influence on mechanical and performance properties. Increasing efforts have been made to predict direct maps of grain structures formed during solidification process. Deterministic models[1,2] couple the heat flow equation at the scale of the whole process with the phenomenological laws describing the nucleation and growth of grains. As a result of these models, the average size of equiaxed grains or even the longitudinal extension of columnar grains can be obtained. The phase-field method presented by Karma and Rappel[3] can be used to simulate the 3D growth morphology of equiaxed dendrites and their branching details[4,5]. Spittle and Brown[6], Zhu and Smith[7] adopted Monte Carlo method for the prediction of grain structures in casting. Rappaz and Gandin[8,9] introduced a physically based cellular automaton approach, which integrated a growth kinetics model and the preferential growth direction of dendrites[10,11].

Considering the advantage of the above methods, a stochastic modeling, based on CA method, was presented for simulating the evolution of dendritic grains during the solidification process of aluminum alloy.

2 MATHEMATICAL MODEL FOR MICROSTRUCTURE SIMULATION

2.1 Nucleation model

Continuous nucleation model was used to describe the nuclei formation during solidification. The density of grains at a given undercooling is given by the integral of nucleation density distribution[1,8]:

$$n(\Delta T) = \int_0^{\Delta T} \frac{\mathrm{d}n}{\mathrm{d}(\Delta T')}\mathrm{d}(\Delta T') \tag{1}$$

$$\frac{\mathrm{d}n}{\mathrm{d}(\Delta T')} = \frac{n_{\max}}{\sqrt{2\pi}\Delta T_\sigma}\exp\left[-\frac{1}{2}\left(\frac{\Delta T' - \Delta T_N}{\Delta T_\sigma}\right)^2\right] \tag{2}$$

where ΔT_N is the mean nucleation undercooling, ΔT_σ is the standard deviation, $n_{\max}$ is the total density of grains.

When the temperature is lower than the liquidus, the density of new grains is given by

$$\delta n = n[\Delta T + \delta(\Delta T)] - n(\Delta T) = \int_{\Delta T}^{\Delta T+\delta(\Delta T)} \frac{\mathrm{d}n}{\mathrm{d}(\Delta T')}\mathrm{d}(\Delta T')$$

The number of new grains in this time-step is given by the multiplication of the grain density increase δn with the total volume of the melt, $\delta N = \delta n \cdot V$. The location of these new grains is randomly chosen among the liquid micro-cells.

2.2 Crystal growth model

2.2.1 Physical model

Under non-equilibrium condition, the solute gradient in front of the edge and corners of the polyhedron is higher, which leads to rapid diffusion of solute and rapid growth at the edge and corner, hence the crystal grain grows from equilibrium polyhedron to

① **Foundation item:** Project (59990470-3) supported by the Significant Project of NSF of China; project(G2000067208-3) supported by the National Significant Fundamental Research Project of MOST of China; project supported by Tsinghua University

Received date: 2003-02-20; **Accepted date:** 2003-07-04

Correspondence: XU Qing-yan, Associate professor, PhD; Tel: +86-10-62789922; Fax: +86-10-62770190; E-mail: scjxqy@tsinghua.edu.cn

asterisk, and then to dendritic[12]. Because of the complexity of equiaxed dendrite, tertiary and the above arm branching are not considered here, the grain shape can be simplified as Fig. 1.

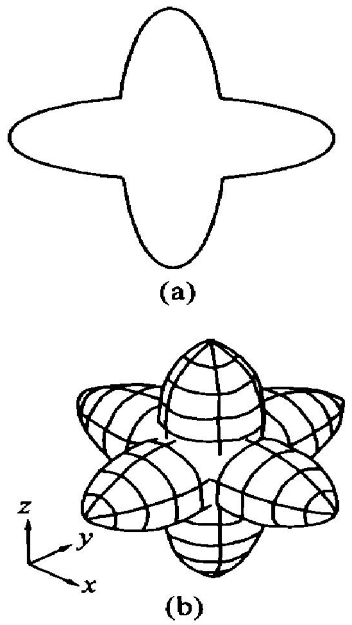

Fig. 1 Simplified grain shape
(a) —2D shape; (b) —3D solid (shaded image)

The following function $L(\theta)$ was defined for 2D shape:

$$L(\theta)=L_0[A+(1-A)\cos 4\theta]$$

The factor A determines the anisotropy of the shape function. The minimum value of A is 0.5, and a circular shape with A of 1 can describe the cellular growth. L_0 can be calculated with the numerical method during the growth. Therefore, the shape of the dendrite will be determined by the factor A, which depends on the growth conditions, the diffusion coefficient and surface energy. Under the condition of high thermal gradient and low cooling rate, tertiary arms could be neglected, so the shape function is a good geometric approximate approach.

For 3D, the following equations can be used to represent the grain contour:

$$\begin{cases} X^2=L_{1a}^2-\Phi_{1a}^2(Y^2+Z^2) & (X\geqslant 0)\\ X^2=L_{1b}^2-\Phi_{1b}^2(Y^2+Z^2) & (X<0)\\ Y^2=L_{2a}^2-\Phi_{2a}^2(X^2+Z^2) & (Y\geqslant 0)\\ Y^2=L_{2b}^2-\Phi_{2b}^2(X^2+Z^2) & (Y<0)\\ Z^2=L_{3a}^2-\Phi_{3a}^2(X^2+Y^2) & (Z\geqslant 0)\\ Z^2=L_{3b}^2-\Phi_{3b}^2(X^2+Y^2) & (Z<0) \end{cases}$$

where L_{1a}, L_{1b}, L_{2a}, L_{2b}, L_{3a} and L_{3b} are the dendrite radii along six directions respectively (seen in Fig. 2); Φ_{1a}, Φ_{1b}, Φ_{2a}, Φ_{2b}, Φ_{3a} and Φ_{3b} are the shape factors related to the average solid fraction and can be defined as follows:

$$\Phi=Z/X_{\rm tip} \tag{6}$$

The representation of Z and $X_{\rm tip}$ can be seen in Fig. 2. From Li and Beckermann's research[13], there is a relation between the growing parameters of dendrite tip as follows:

$$X_{\rm tip}/R=0.668(Z/R)^{0.859} \tag{7}$$

This experimental correlation is valid in the self-similar regime given by $1\ll Z/R\ll 1/Pe$.

Then

$$\Phi=1.497(Z/R)^{0.141} \tag{8}$$

2.2.2 Numerical model

The schematic representation of equiaxed grain growth model is shown in Fig. 3. A is a nucleation site in mesh grids which is nucleated at a certain time $t_{\rm N}$. At time t, the radius of grain $L(t)$, is the integral along the whole growing time:

$$L(t)=\int_V v[\Delta T(t')]\,{\rm d}t' \tag{9}$$

$v[\Delta T]$ can be calculated by KGT model. At the time t_1, the grain A grows and touches the four neighboring cells $B1-B4$. Then $B1-B4$ are considered to become solid and assigned a crystallographic index same as A. The grain continues to grow and capture the other neighboring sites at next time t_2, etc. On growing, each grain continues to capture the nearest neighbor cells and form the final grain shape. When a neighboring cell has been captured by other grains, the growth along this direction stop, which

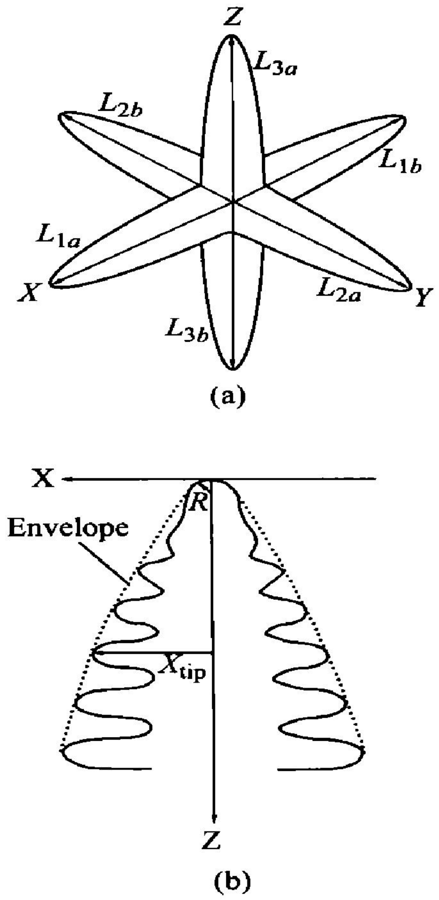

Fig. 2 Growth radius of grain (a) and sketch map of dendrite tip (b)

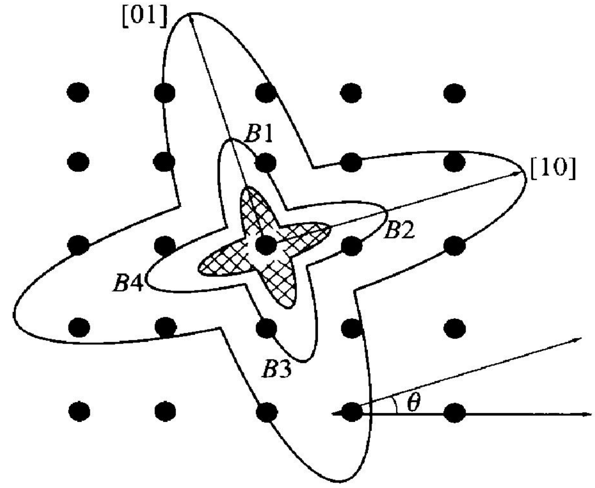

Fig. 3 Grain growth model for equiaxed grain.

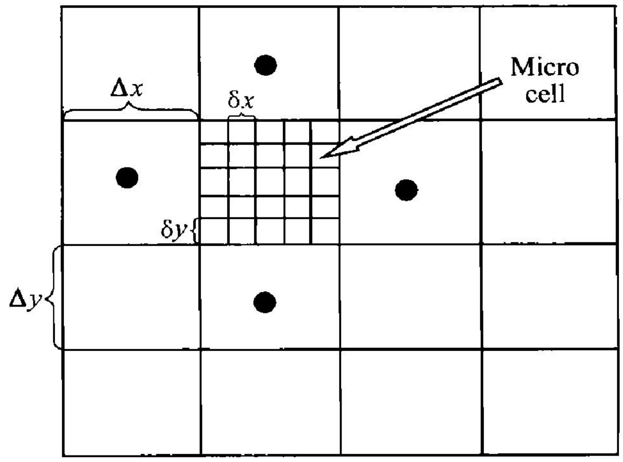

Fig. 4 Schematics for macro and micro cells

reflects the grain impingement phenomenon occurring in solidification process.

2.3 Computing model

For most metallic alloys thermal and kinetic undercooling have little effect on the total undercooling, the constitutional and curvature undercooling are the predominant under normal casting condition. Therefore

$$\Delta T = T_l^{EQ} + (c_l^* - c_0) m - \Gamma K - T^* \qquad (10)$$

where T_l^{EQ} is the equilibrium liquidus temperature of the alloy; m is the liquidus slope of the phase diagram; K is the mean curvature of the solid/liquid interface; Γ is the Gibbs-Thomson coefficient; c_l^* is the solute concentration at the solid/liquid interface; c_0 is the initial concentration of the alloy in the liquid; and T^* is the temperature at the interface.

$$c_l^* = c_0(1 - f_s)^{k-1} \qquad (11)$$

$$K = \frac{1}{l}\left(1 - 2\frac{f_s + \sum_{i=1}^{N} f_s(i)}{N+1}\right) \qquad (12)$$

where l is the mesh length of micro-cells, and N is the number of neighboring cells[14].

The growth velocity of dendrite tip can be calculated by KGT model, which is widely used in the micro-modeling. The details can be seen in Refs. [8-11].

3 COUPLING CALCULATION OF MACRO/MICRO MODELING

Different time and space steps were used for macro and micro modeling, where Δx and Δt are macro step and δx and δt are micro (Fig. 4). A macro grid is divided into several micro cells. Usually Δx is about several mm and δx about several μm. Δt must meet a need of stability condition, which is determined by heat transfer equations and boundary conditions, in the scale of 0.1 s to 0.0001 s. Micro time step δt is controlled by nucleation and growth iterative computation and at about 10^{-6} order of magnitude.

Due to the small size of the micro-cell, it will take much more time to calculate the temperature of all micro-cells by numerically solving the heat transfer equation. For example, for a 10 mm × 10 mm × 10 mm cubic casting, in order to simulate the dendrite growth the side length of a cell may be 2 μm and the total cells number can be up to 2.5×10^7 for 2D and 1.25×10^{11} for 3D. Moreover, the real casting is much larger than this scale. So the computing amount is very large.

Obviously, the temperature of a micro cell is influenced by its nearest neighboring macro-cells, and hence the interpolation formula can be constructed according to the thermal contribution of macro-cells, i.e. the temperature of the micro cell is in reverse ratio to the distance between the neighboring macro-cell and point a:

$$T_a = \sum_{i=1}^{4} l_i^{-1} T_i \Big/ \sum_{i=1}^{4} l_i^{-1} \qquad (13)$$

where T_a is the temperature of the micro cell a, T_i is the temperature of the neighboring macro-cell, and l_i is the distance from a to the macro-cell.

The flowchart for macro/micro coupling scheme of microstructure simulation is shown in Fig. 5. It can be seen that only macro calculation is carried out when the temperature is higher than liquidus. When the temperature is between the liquidus and solidus macro and micro modeling are coupled. During the computing, the temperature of the micro cells is interpolated by those of neighboring macro-cells. The latent heat released by the solidified micro cells is transferred to the macro heat transfer calculation. By this means, the macro heat transfer is coupled with the micro modeling.

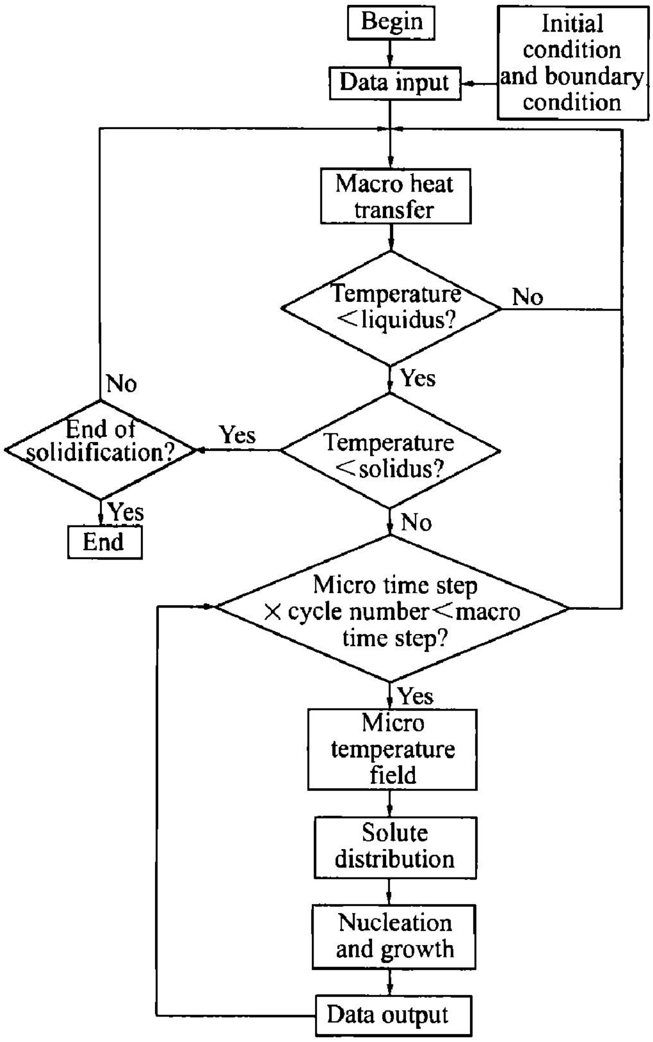

Fig. 5 Flowchart for macro-micro coupling scheme of microstructure simulation

4 VALIDATION EXPERIMENTS

In order to validate the modeling results, some experiments were carried out. The sample shape and size are schematically shown in Fig. 6. Step-shaped samples were poured with A356 alloy into sand mold. The experimental condition is shown in Table 1. The specimens were taken from the center part of the sample castings and observed with an optical microscope after polishing and etching.

5 RESULTS AND DISCUSSION

Microstructure calculation scheme and post-processing module were developed based on the above algorithm. The grain structure prediction of A356 alloy was carried out and the thermophysical parameters used in the calculation are listed in Table 2.

5.1 Modeling of free growth of equiaxed grain

In order to simulate free dendritic growth into

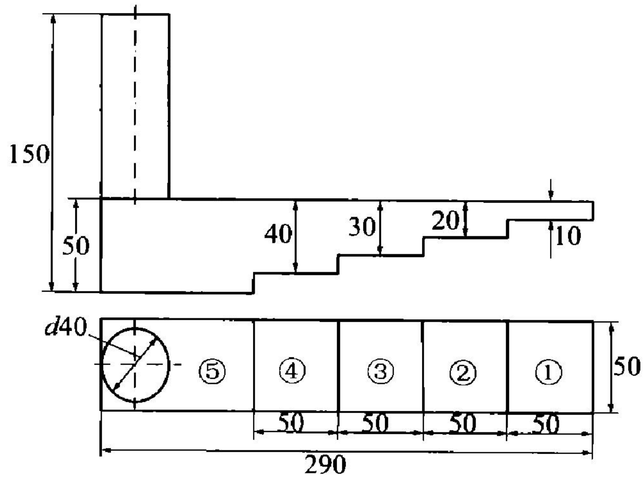

Fig. 6 Sample shape and positions for modeling

Table 1 Experimental conditions

Material	Casting method	Pouring temperature	Room temperature
A356	Sand mold	700 ℃	25 ℃

Table 2 Thermophysical properties of A356 alloy

Thermal conductivity W/(m·℃)	Specific heat [J/(m^3·℃)]	Latent heat/ (J/m^3)
125	2.96×10^6	9.5×10^8

Liquidus/ ℃	Solidus/ ℃	Partition coefficient/ K	Slope of liquidus/ (℃/%)
614	542	0.117	−6

an undercooled melt, the calculating domain is divided into 120 × 120 × 120 cells with a cell size of 1 μm. The undercooling is 10 K. Assume that the grain growth direction along the coordinate axis is zero. The modeling results are shown in Fig. 7.

5.2 Modeling of growth of multi-grains

Fig. 8 shows the evolution of the grain structure during solidification. The number of grid points used in calculation is 500 × 500, and the size is $dx = dy =$ 20 μm.

The growth of multi grains was simulated with the 3D simplified model under the parallel computing environment. The modeling results are shown in Fig. 9. In this model the nucleus position and growth orientation are both random which agrees with the physical mechanism.

5.3 Modeling of grain structures of Al alloy casting

The size of macro-cell for the calculation of heat transfer is 2 mm × 2 mm × 2 mm, which is further divided into 500 × 500 × 500 micro cells. The microstructures at positions ①, ②, ③, ④and ⑤were calculated respectively. Fig. 10 shows the comparison of modeling results and the metallo

Fig. 7 Free growth of equiaxed grain in undercooled melt

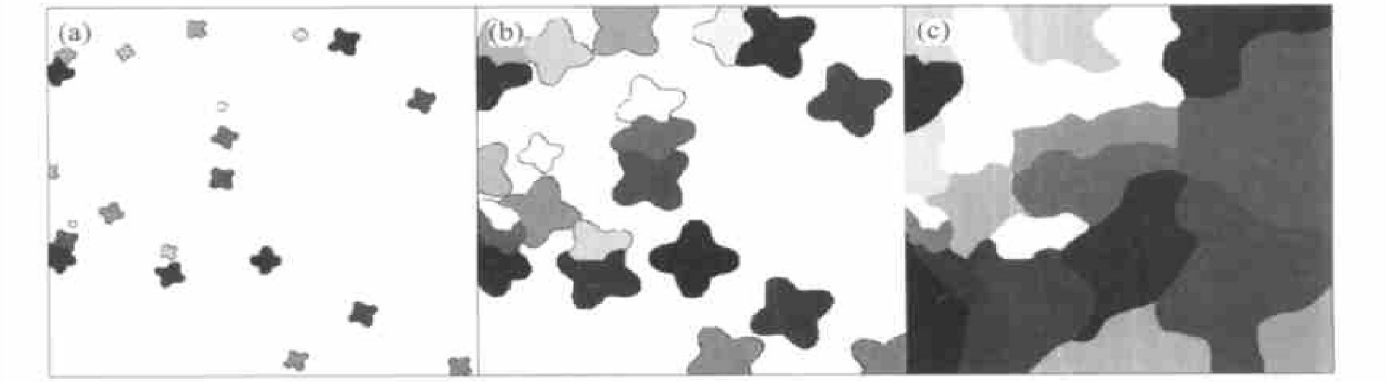

Fig. 8 Formation of equiaxed grains in undercooled melt at different solidification times
(a) —t= 0.06 s; (b) —t= 0.08 s;

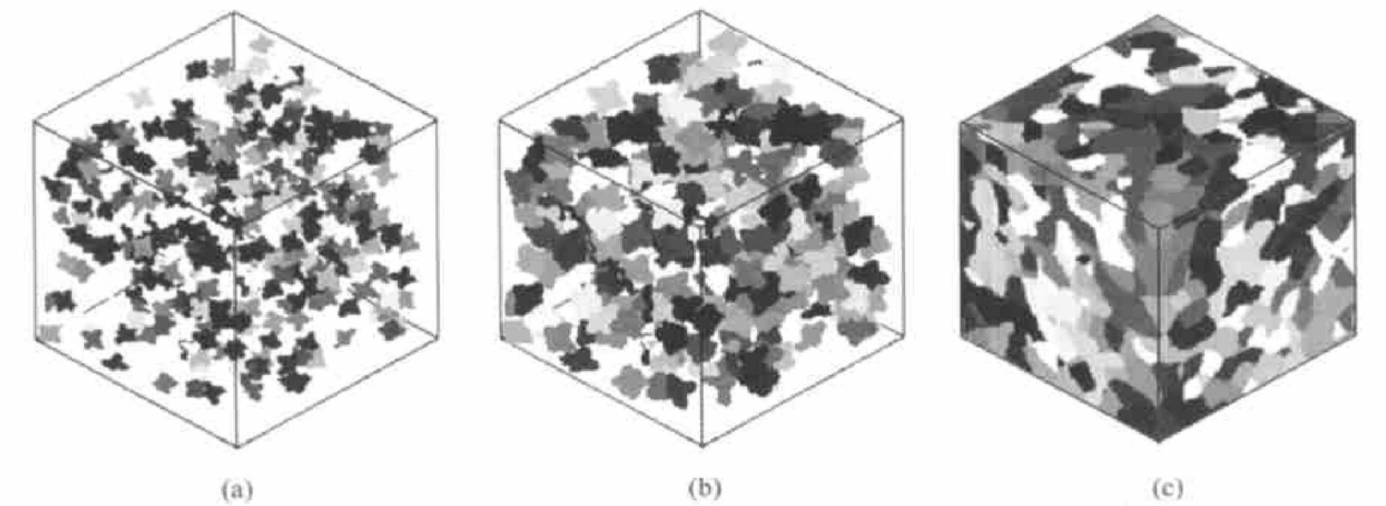

Fig. 9 Modeling results using 3D simplified dendrite model
(a) —t= 0.01 s; (b) —t= 0.04 s;

graphs for sand mold. In Fig. 10, (a) refers to the position of sample, (b) is the 3D modeling results, (c) is the 2D section of 3D results, (d) is the experimental metallographs of real castings. It can be seen that the modeling image is similar with the observed metallographs. Quantitative metallurgical analysis also has been done. The calculated and real grain size is listed in Table 3, which is very close between the modeling and measured value.

6 CONCLUSIONS

1) Simplified physical and mathematical models for microstructure simulation were established , in which shape functions were constructed to describe the approximate contour of dendritic grain. Based on the above models, the equiaxed grain growth model was proposed to depict the grain growing process and

Table 3 Calculated and measured grain sizes

Position	Measured cooling rate/ (℃·s^{-1})	Grain size/ mm	
		Measured	Calculated
1	0.30	0.143	0.140
2	0.27	0.172	0.181
3	0.23	0.201	0.210
4	0.19	0.245	0.239
5	0.15	0.271	0.265

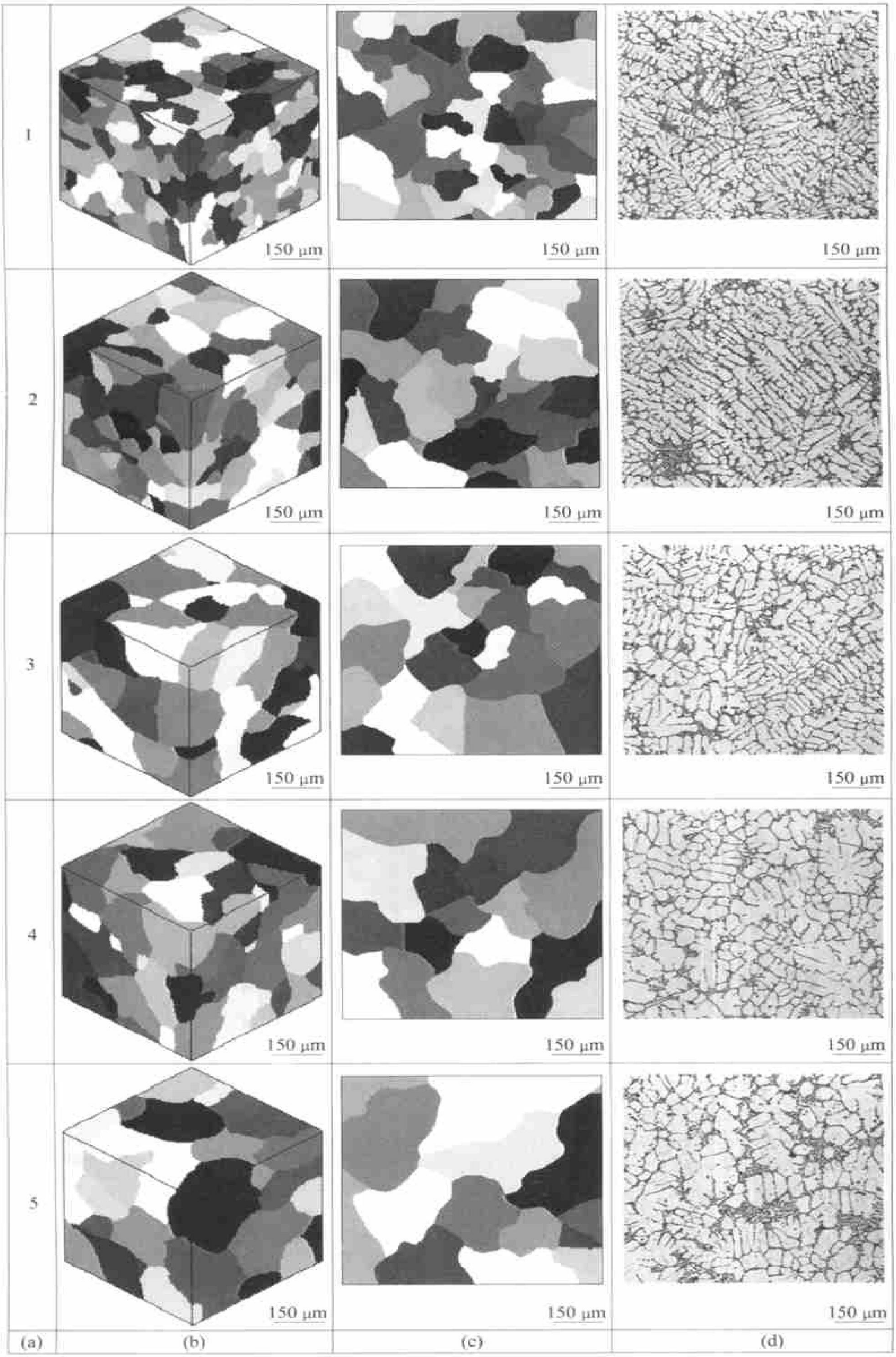

Fig. 10 Comparison between experimental and simulated results
(a) —Position; (b) —3D modeling results; (c) —2D section of 3D image; (d) —Experimental micrograph

capture other grid nodes during the further growth.

2) A stochastic modeling method was proposed to model the equiaxed dendritic grain formation of Al alloy during the solidification, in which the simplified dendritic shape was used to represent the growing grain. 2D and 3D modeling calculations were performed for step-shaped casting of aluminum alloy. It is indicated that the calculated grain size coincides with the experimental size.

REFERENCES

[1] Rappaz M. Modeling of microstructure formation in solidification processes[J]. Inter Mater Rev, 1989, 34(3): 93-123.

[2] Zhao H D, Liu B C. Modeling of stable and metastable eutectic transformation of spheroidal graphite iron casting [J]. ISIJ Inter, 2001, 41 (9): 986-991.

[3] Rappel W J, Karma A. Phase-field simulation of three-dimensional dendrites: Is microscopic solvability theory correct? [J]. J Crystal Growth, 1997, 174(1-4): 54-64.

[4] Nestler B, Wheeler A A. Anisotropic multi-phase-field model: Interfaces and junctions[J]. Phys Rev E, 1998, 57(3): 2603-2609.

[5] Zhang G Y, Jing T, Liu B C. Microstructure simulation of aluminum alloy casting using phase field method[J]. Int J Cast Metal Res, 2002, 15(3): 237-240.

[6] Spittle J A, Brown S G R. Computer simulation of the effects of alloy variables on the grain structures of castings [J]. Acta Metall, 1989, 37(7): 1803-1810.

[7] Zhu P, Smith R W. Dynamic simulation of crystal growth by Monte Carlo method-I: model description and kinetics[J]. Acta Metall Mater, 1992, 40(4): 683-692

[8] Rappaz M, Gandin Ch-A. Probabilistic modeling of microstructure formation in solidification process[J]. Acta Metall Mater, 1993, 41(2): 345-360.

[9] Gandin Ch-A, Rappaz M. Coupled finite element-cellular automation model for the prediction of dendritic grain structures in solidification processes[J]. Acta Metall, 1994, 42(7): 2233-2246.

[10] Zhu M F, Hong C P. A modified cellular automaton model for the simulation of dendritic growth in solidification of alloys[J]. ISIJ International, 2001, 41(5): 436-445.

[11] Xu Q Y, Liu B C. Modeling of as-cast microstructure of Al alloy with a modified cellular automaton method[J]. Mater Trans, 2001, 41(7): 2316-2321.

[12] Hu H Q. Solidification Principles of Metals[M]. Beijing: China Machine Press, 2000. 80-90. (in Chinese)

[13] Li Q, Beckermann C. Scaling behavior of three-dimensional dendrites[J]. Physical Review E, 1998, 57(3-B): 3176-3188.

[14] Nastac L. Numerical modeling of solidification morphologies and segregation patterns in cast dendritic alloys [J]. Acta Mater, 1999, 47(17): 4253-4262.

(Edited by PENG Chao-qun)